Observations of a high-latitude stable electron auroral emission at ~16 MLT during a large substorm

C. Cattell,[1] J. Dombeck,[1] A. Preiwisch,[1] S. Thaller,[1] P. Vo,[1] L. B. Wilson III,[1] J. Wygant,[1] S. B. Mende,[2] H. U. Frey,[2] R. Ilie,[3] and G. Lu[4]

Received 17 September 2010; revised 6 April 2011; accepted 20 April 2011; published 19 July 2011.

[1] During an interval when the interplanetary magnetic field was large and primarily duskward and southward, a stable region of auroral emission was observed on 17 August 2001 by IMAGE at ~16 magnetic local time, poleward of the main aurora, for 1 h, from before the onset of a large substorm through the recovery phase. In a region where ions showed the energy dispersion expected for the cusp, strong field-aligned currents and Poynting flux were observed by Polar (at 1.8 R_E in the Southern Hemisphere) as it transited field lines mapping to the auroral spot in the Northern Hemisphere. The data are consistent with the hypothesis that the long-lasting electron auroral spot maps to the magnetopause region where reconnection was occurring. Under the assumption of conjugacy between the Northern and Southern hemispheres on these field lines, the Polar data suggest that the electrons on these field lines were accelerated by Alfvén waves and/or a quasi-static electric field, primarily at altitudes below a few R_E since the in situ Poynting flux (mapped to 100 km) is comparable to the energy flux of the emission while the mapped in situ electron energy flux is much smaller. This event provides the first example of an emission due to electrons accelerated at low altitudes at the foot point of a region of quasi-steady dayside reconnection. Cluster data in the magnetotail indicate that the Poynting flux from the reconnection region during this substorm is large enough to account for the observed nightside aurora.

Citation: Cattell, C., et al. (2011), Observations of a high-latitude stable electron auroral emission at ~16 MLT during a large substorm, *J. Geophys. Res.*, *116*, A07215, doi:10.1029/2010JA016132.

1. Introduction

[2] Many researchers have studied the time variations of the aurora observed in association with substorms, and summaries have been presented by *Akasofu* [1964], *Elphinstone et al.* [1996], and others. The stages of brightening and expansion of the auroral oval during substorms are associated with dramatic changes in the topology of the geomagnetic field and in the plasma regions of the magnetosphere. It is generally accepted that the variability in the observed auroral forms is directly linked to these changes in topology and the associated energy release processes.

[3] In addition to substorm-associated aurora, there are a number of localized features that are observed primarily during quiet times or under specific interplanetary magnetic field conditions. *Frey* [2007] has reviewed those that occur outside the region of the main auroral oval. One of these is the high-latitude dayside aurora (HiLDA), which occurs poleward of the main oval and is sometimes found to occur in the shape of a spot. *Frey et al.* [2003c, 2004] showed that the emissions were due only to energetic electrons and not to protons. Their statistical studies indicated that these spots, which can last for periods of many hours, occurred primarily during northward interplanetary magnetic field (IMF) and low solar wind dynamic pressure. The magnetic local time of the spots was correlated with the *y* component of the IMF. On the basis of comparisons of the images to in situ FAST observations of currents and particles and assimilative mapping of ionospheric electrodynamics (AMIE) model calculations of the currents, *Frey et al.* [2003c] concluded that the emissions occurred in the region of upward field-aligned current closing the downward current associated with the adjacent cusp precipitation at lower latitude.

[4] A number of authors [*Fuselier et al.*, 2002; *Frey et al.*, 2002] have described the occurrence of auroral spots, observed by the IMAGE SI12 camera, due to protons on field lines associated with dayside reconnection during northward IMF. *Phan et al.* [2003] showed that the ions producing the emission were accelerated via reconnection in the high-latitude magnetopause [*Phan et al.*, 2003, Figure 3]. *Frey*

[1]School of Physics and Astronomy, University of Minnesota, Twin Cities, Minneapolis, Minnesota, USA.
[2]Space Sciences Laboratory, University of California, Berkeley, California, USA.
[3]Department of Atmospheric, Oceanic and Space Sciences, University of Michigan, Ann Arbor, Michigan, USA.
[4]High Altitude Observatory, National Center for Atmospheric Research, Boulder, Colorado, USA.

0148-0227/11/2010JA016132

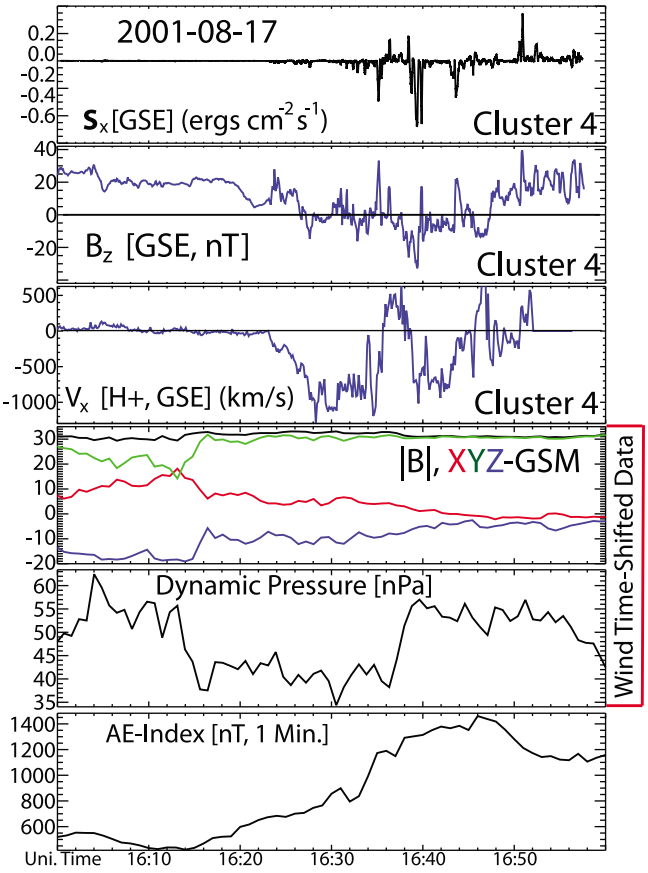

Figure 1a. The *x*-GSE component of the Poynting flux (first panel), the *z*-GSM component of the magnetic field (second panel), and the GSE *x* component of the ion flow velocity from Cluster 4 from 16:00 to 17:00 UT (third panel); the three components of the magnetic field (fourth panel) and the dynamic pressure from Wind (lagged to the magnetopause) (fifth panel); and the *AE* index (sixth panel).

et al. [2003b] extended the study to cases with southward IMF. The emission brightness was shown to depend on solar wind dynamic pressure.

[5] On 17 August 2001, the Cluster satellites, located at ~18 R_E near midnight local time, observed the signature of the initiation of reconnection at the same time as the brightening of the nightside aurora was observed by IMAGE and as *AE* increased in association with the onset of a substorm. In this report, we examine a long-lived dayside auroral emission spot, poleward of the main oval at ~16 magnetic local time (MLT), which was observed before, during, and after the onset of this intense substorm. Despite the dramatic changes in magnetic field topology on the nightside associated with substorm reconnection, the location of the spot did not change, although the brightness did, suggesting that the dynamics in this afternoon local time region were not strongly influenced by the substorm. Data from the IMAGE FUV camera, together with ACE and Wind data, are used to examine the dependence of the emission on solar wind parameters. It will be shown that this auroral spot has distinctly different characteristics from those previously reported and summarized above. Data from the Polar satellite in the Southern Hemisphere at ~1.8 R_E, on field lines mapping to the emission spot observed in the Northern Hemisphere, are used to elucidate energy flow and the acceleration of the auroral electrons. Data assimilation and MHD models provide additional information on mapping and context.

2. Data Sets, Solar Wind Conditions, and Magnetic Activity

[6] Data sets from five spacecraft missions were utilized to examine the timing of changes in the aurora, in the magnetotail, and on auroral field lines for this event. Electric field and spacecraft potential measurements from the double probe electric field instrument (EFW) [*Gustafsson et al.*, 1997], magnetic field measurements from the fluxgate magnetometer (FGM) instrument [*Balogh et al.*, 2001], and plasma flows from the Cluster Ion Spectrometry (CIS) instrument [*Réme et al.*, 1997] from the Cluster satellites provided information on the onset of reconnection and the associated energy flow in the magnetotail. EFW measured the electric field in the satellite spin plane (approximately the GSE *x*-*y* plane) with a time resolution of 25 samples/s for this event. FGM obtained a full three-dimensional measurement of the magnetic field at 20 samples/s. CIS provided ion moments at spin period resolution (4 s).

[7] Observations of the auroral emissions were made by the wideband imaging camera (WIC) from the FUV instrument on IMAGE [*Mende et al.*, 2000]. The SI12 images were also examined to provide information on proton aurora. During the interval of interest, aurora in the Northern Hemisphere was monitored. The Polar satellite was in the Southern Hemisphere at an altitude of 1.8 R_E. As will be discussed in section 3, tracing of the Polar field lines to the Northern Hemisphere indicates that Polar was conjugate to the auroral emission of interest. The full three-dimensional electric field was measured by the double probe electric field instrument [*Harvey et al.*, 1995] at a rate of 20 samples/s. The spin axis component of the field is measured by shorter (13.8 m) booms than the spin plane components (100 m and 160 m). For the event herein, only the spin plane data are utilized to examine the Poynting flux. The three-dimensional magnetic field, filtered at 4 Hz, is obtained at a rate of 8.3 samples/s by the magnetic field experiment [*Russell et al.*, 1995]. Plasma observations are made by HYDRA [*Scudder et al.*, 1995] and provide electron and ion distributions with a 13.8 s resolution.

[8] Interplanetary conditions were obtained from the ACE and Wind satellites and time-lagged to the magnetopause. High densities (~20–30/cc) and moderate speeds (470–500 km/s) were observed, the dynamic pressure was large (~10 nPa), and conditions were quite stable during the hour of interest (see Figure 1a). The total magnetic field was ~35 nT, dominantly in the positive *y*–negative *z* (duskward and southward) direction, throughout most of the interval. The interval of interest occurred in association with the onset of a large substorm (peak *AE* ~1400 nT) and near a storm onset, at a time when *Dst* was ~13 nT, associated with storm sudden commencement compression.

[9] In addition to the satellite observations, results from the Space Weather Modeling Framework (SWFM) global MHD model [*Tóth et al.*, 2005; *Gombosi et al.*, 2001] obtained

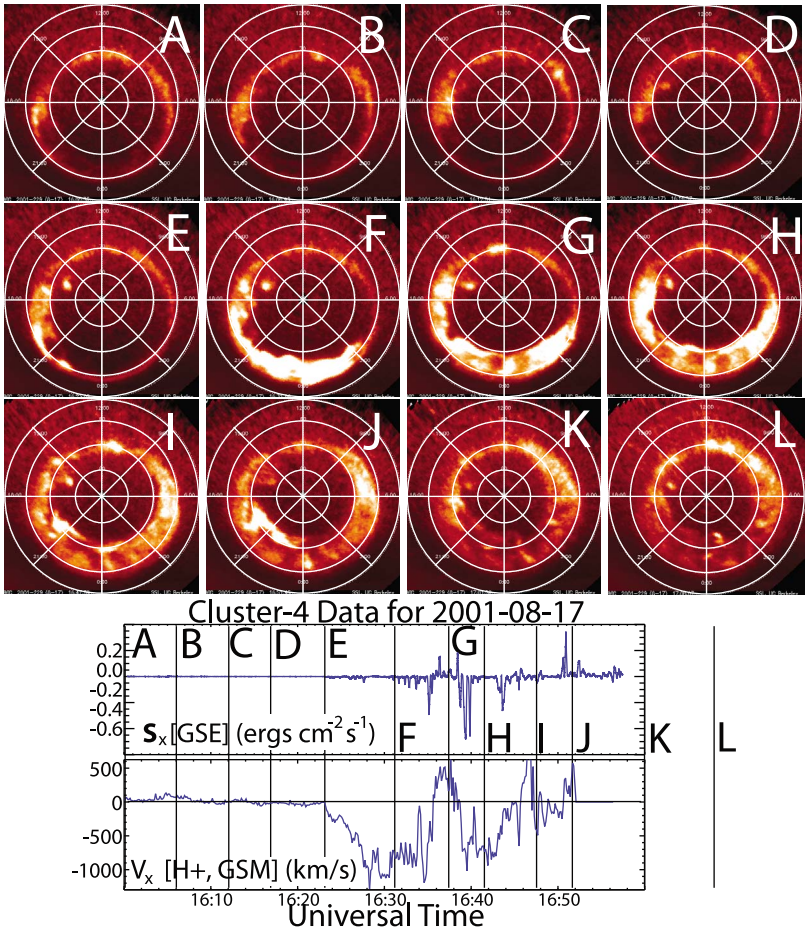

Figure 1b. (top) Selected images from the WIC instrument on IMAGE. The invariant latitude (ILAT) lines are at 10° intervals from 50° to 80°; the MLT lines are at 3 h intervals with 12 MLT at the top and 18 MLT at the left of each image. (bottom) The x component of the Poynting flux and the x component of the plasma velocity from Cluster 4. Vertical lines and letters indicate the times of the images. Note that the images labeled K (at 17:01 UT) and L (at 17:08 UT) occurred after the end of the available Cluster data.

for this substorm and calculations from the AMIE model [*Richmond*, 1992; *Richmond et al.*, 1998] are utilized to provide context, information on likely mapping of regions in the ionosphere and at low altitudes to the outer magnetosphere, as well as synoptic information on large-scale currents.

3. Observations

[10] On 17 August 2001, the Cluster satellites were at a radial distance of ~18 R_E near 1 MLT when they detected the signature of reconnection associated with substorm onset. Figure 1a presents (from top to bottom) the x-GSE component of the in situ Poynting flux, the z-GSM component of the magnetic field and the GSE x component of the ion flow velocity from Cluster 4 from 16:00 to 17:00 UT, the three components of the magnetic field and the dynamic pressure from Wind (lagged to the magnetopause), and the *AE* index. The typical signature of near-Earth reconnection [*Hones*, 1976], tailward flow associated with southward B_z, can be seen. The fast tailward flow began at ~16:23 UT at Cluster 4 and continued until ~16:45 UT, with a brief change to earthward flow at ~16:36 UT. The in situ value of the Poynting flux is also shown, indicating energy flow away from the reconnection x line. In the region of earthward flow and positive B_z, i.e., on field lines connected to the Earth, the Poynting flux is also earthward with a peak in situ (mapped to 100 km) magnitude of ~0.2 mW/m^2 (200 mW/m^2). Examination of the Poynting flux measured on the other three Cluster satellites shows comparable magnitudes, indicating that the strong Poynting flux occurs over regions at least as large as the satellite separations of ~1000 km. The interplanetary magnetic field was very steady during this 1 h interval with large positive B_y (~30 nT) and negative B_z (~10 nT). The dynamic pressure was also large with the variability due almost entirely to changes in the density (from ~20/cc to ~28/cc).

[11] Prior to the onset of fast tailward flow at Cluster and the increase in the *AE* index, the ultraviolet images of the global aurora, made by the WIC on IMAGE (Figure 1b),

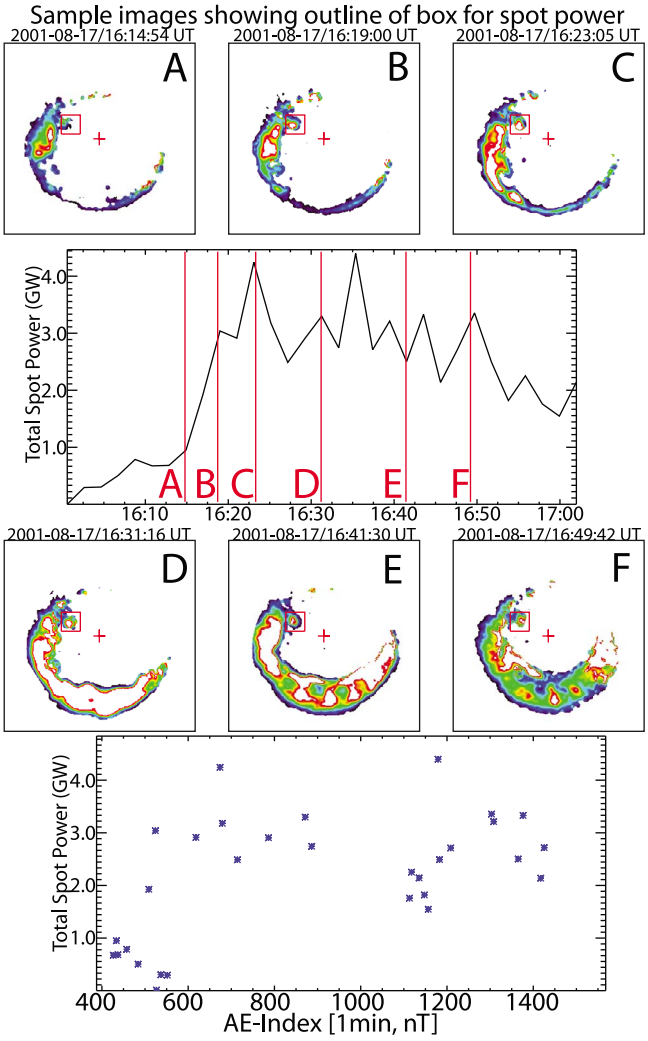

Figure 2. The first and third rows show sample WIC images (color indicates energy flux) with the box over which the total power in the spot was obtained plotted in red. Note that the orientation (MLT and ILAT) is identical to that of the images in Figure 1b. The second row is the total power in the spot versus time. The fourth row plots the total power in the spot versus *AE*.

showed a broad region of emission on the dayside and only very weak emission, narrow in latitude, on the nightside. At approximately the time of the onset of fast flow and observable Poynting flux at Cluster, the aurora on the duskside brightened. The typical progression of the nightside aurora through the course of a substorm occurred. In addition, a very stable spot at approximately 16 MLT and 76° invariant latitude (poleward of the main oval) can be seen prior to substorm onset and throughout the duration of the substorm from ~16:08 to ~17:10 UT. Although the feature brightens in concert with the substorm-associated brightening in the rest of the oval, its position does not change. No emissions were observed at the location of the spot in the IMAGE SI12 camera images, indicating that the emissions were solely an electron feature.

[12] No specific changes in the solar wind parameters were observed at the time the spot first became visible; however, the total power in the spot began to increase at ~16:12 UT in association with a slight decrease in solar wind dynamic pressure and the magnitude of the southward IMF B_z and increase in IMF B_y (see Figures 1a and 2). The decrease in brightness and eventual disappearance of the spot was associated with either northward or only weakly southward B_z and a large decrease in solar wind pressure. To examine in more detail the dependence of the power in the spot on solar wind parameters and on magnetic activity, the peak energy flux and total power in an area around the spot was determined for each image during the 1 h interval from 16:00 to 17:00 UT. Figure 2 shows several of the mapped images; the red boxes indicate the area over which the averaging was done (the same area was used for each image). The total power versus time for all images in the 1 h interval is plotted in the second row in Figure 2. There were no correlations found between the total power or the peak energy flux and solar wind dynamic pressure, density, IMF B_z, IMF B_y, or $E_{\text{solar wind}}$. The fourth row in Figure 2 shows that there was only a very weak relationship between brightness and the *AE* index; that is, the lowest power occurred when *AE* was smallest.

[13] At ~16:23 UT, the Polar satellite, at ~1.8 R_E in the Southern Hemisphere, passed through field lines that were approximately conjugate to the spot IMAGE observed in the Northern Hemisphere. Figure 3 plots, from top to bottom, the field-aligned (away from Earth) and anti-field-aligned (toward Earth) electron energy fluxes, the ion field-aligned and anti-field-aligned energy fluxes, the electron and ion kinetic energy fluxes (negative is earthward), the perpendicular spin plane component of the quasi-static electric field, the azimuthal (spin axis) magnetic field perturbation, and the field-aligned Poynting flux (positive is earthward). The downgoing ion data show a steep energy dispersion with latitude, consistent with that expected for the cusp [*Reiff et al.*, 1977; *Smith and Lockwood*, 1996]. The large upward field-aligned current (positive slope in the azimuthal dB), ion and electron kinetic energy fluxes, and Poynting flux occur at the inner edge of this region at the boundary between magnetospheric and magnetosheath particles. The mapped location of Polar has also been determined by tracing field lines in the SWFM run for this substorm. This mapping, shown in Figure 4, clearly shows that Polar is on the field line that maps to the equatorial magnetopause at the time of the large electric and magnetic field signature, consistent with the interpretation of the ion dispersion. The mapping to the Northern Hemisphere utilizing the Tsyganenko 89, 96, 01, and 04 models also is consistent with Polar being conjugate to the spot. The scale size of the region of enhanced Poynting flux is comparable to the size of the spot.

[14] The maximum value of the electron kinetic energy flux, mapped to 100 km, observed by Polar in the Southern Hemisphere was ~1.2 mW/m^2, more than an order of magnitude lower than the peak energy flux observed by WIC in the spot in the Northern Hemisphere. With the assumption that the processes on these field lines are conjugate in the Northern and Southern hemispheres, we can conclude that acceleration must have occurred between Polar altitudes and the ionosphere. The Poynting flux obtained from the full resolution data, shown in Figure 3, had peak values of ~400 mW/m^2, which are more than enough to provide the

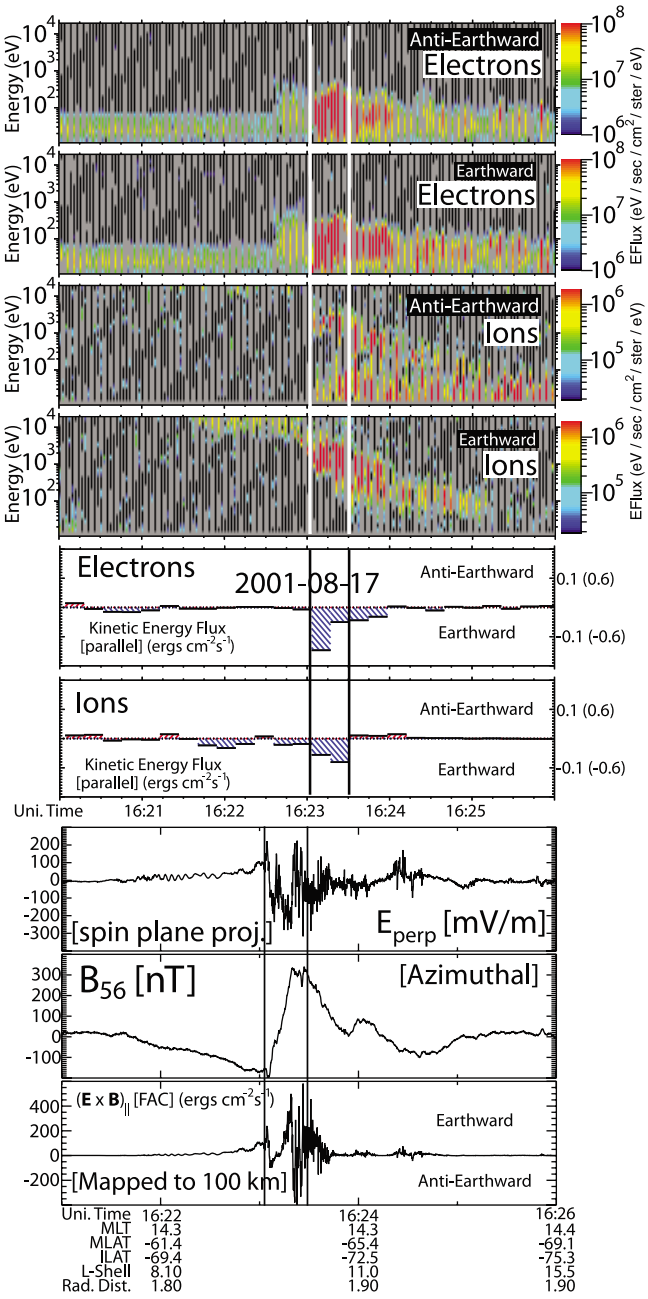

Figure 3. Data from the Polar satellite: the field-aligned (away from Earth) and anti-field-aligned (toward Earth) electron energy fluxes and the ion field-aligned and anti-field-aligned energy fluxes (top four rows). The electron and ion kinetic energy fluxes (middle two rows). (The label shows the in situ value with the mapped value in parentheses.) The perpendicular quasi-static electric field (at full resolution of 20 samples/s), the azimuthal magnetic field perturbation (at full resolution of 8.3 samples/s), and the field-aligned Poynting flux mapped to 100 km (bottom three rows). The vertical lines outline the region of the upward current.

energization of the electrons in the observed auroral emission. There have been many studies of the altitude range over which auroral acceleration occurs, both in quasi-static parallel potential drops and double layers [see, e.g., *Paschmann et al.*, 2003; *Morooka and Mukai*, 2003; *Hull et al.*, 2003; *Ergun et al.*, 2004] and via kinetic/inertial Alfvén waves [*Chaston et al.*, 2002, 2003; *Dombeck et al.*, 2005]. These studies indicate that significant electron acceleration can occur below ~2 R_E, consistent with our interpretation for this event. Although we can infer that the Alfvén waves were propagating along the length of the field line from the magnetopause, the conditions for efficient electron acceleration are expected to occur primarily at lower altitudes in the region of the peak and large gradients in the Alfvén speed [*Goertz and Boswell*, 1979; *Lysak*, 1991; *Kletzing*, 1994; *Lysak and Lotko*, 1996].

[15] To characterize the wave signatures, the electric and magnetic field perturbations have been examined over two time scales: ~10–60 s plotted in Figure 5a and ~1–10 s plotted in Figure 5b. For time scales of 10 to 60 s, the large-scale Poynting flux, defined as that obtained from the 10 s average, is into the ionosphere and has a peak mapped magnitude of 125 mW/m^2. The ratio of the perpendicular electric field to the perpendicular magnetic field perturbation (dE/dB) (see Figure 5a) is ~500 km/s, which is consistent with closure through the ionosphere for expected values for the Pederson conductivity [*Wygant et al.*, 2000; *Paschmann et al.*, 2003; *Dombeck et al.*, 2005]. For the waves with time scales of 1 to 10 s (Figure 5b), dE/dB is ~5000 to 10,000 km/s, which is comparable to the Alfvén speed, and the Poynting flux is ~40 mW/m^2. There are also waves at higher frequencies (~0.1–1 s) with similar electric to magnetic field ratios, consistent with kinetic Alfvén waves [*Lysak and Lotko*, 1996; *Wygant et al.*, 2002]. The Poynting flux observed at Polar is large enough to account for the increase in the electron energy flux needed to account for the observed emissions, as well as the observed perpendicular ion heating and reasonable estimate of Joule heating in the ionosphere.

[16] Qualitative comparisons were made between the observed large-scale vector magnetic field perturbation (not shown) and a limited set of model field-aligned current configurations. Sheet currents and configurations of one, two, and three line currents were tested. The signature is not consistent with a current sheet or sheets extensive in longitude. The closest match was to a configuration consisting of a large upward line current in the center with smaller downward line currents on either side. The inferred line current structure is consistent with the fact that the aurora on the field line were in the shape of a spot rather than extensive in longitude.

[17] The AMIE model results (not shown) indicate the existence of a stable feature in the upward field-aligned current in the Northern Hemisphere in the ~15–16 MLT sector, peaking at ~73°–74°. The largest current was approximately 3–4 μA/m^2, with peak values occurring in the same LT range as the strong emission in the spot. Note, however, that the latitudinal size of the current seen in AMIE is larger than the combined width of the three currents seen by Polar. In the plots of ionospheric parameters from SWFM, there are no clear signatures that can be uniquely associated with the persistent auroral spot observed by IMAGE in the Northern Hemisphere or with the field-aligned current observed by Polar, although there is a peak in the Pederson conductivity at approximately the same LT and invariant latitude and a peak in the electric field that is

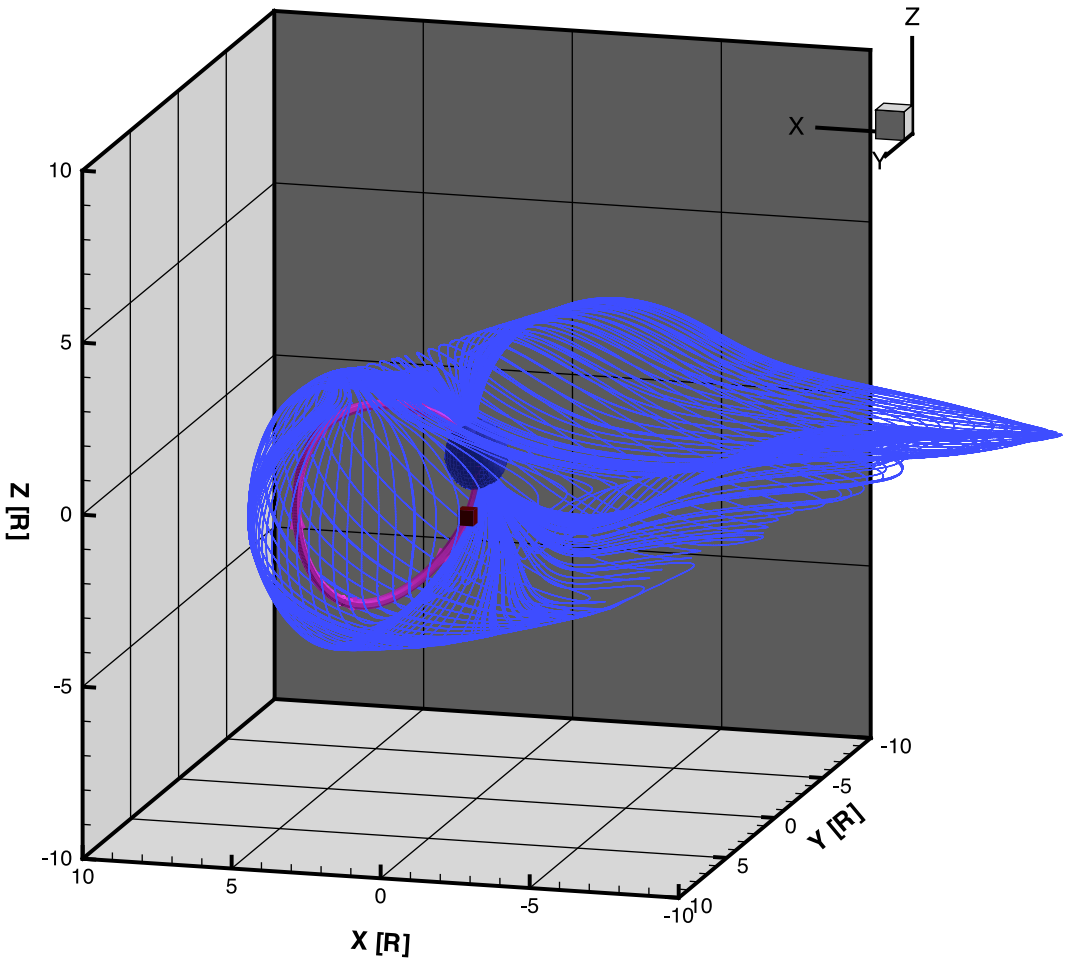

Figure 4. Magnetic field line through the location of Polar at 16:20 UT, plotted in purple, and magnetopause field lines, in blue, from the SWMF simulation for this event.

wider in local time. It is likely that the both the field-aligned current and the auroral spot are too small scale to be resolved in the simulations by AMIE.

4. Discussion and Conclusions

[18] The event described herein is a long-lived (~1 h) auroral emission spot, on the order of a degree in radius, which occurred poleward of the main auroral oval near ~16 MLT. The emission was observed in the IMAGE WIC detector and not in the SI12 imager and thus was due solely to electrons. Although there were very dramatic changes in the aurora at other local times and latitudes, the spot only changed in brightness, generally in concert with the brightness in the main oval. The Polar satellite was in the Southern Hemisphere and traversed the field lines mapping to the corresponding region of the emission observed by IMAGE in the Northern Hemisphere. At this time, the signatures of large field-aligned currents and Poynting flux, both Alfvénic and quasi-static, occurred in association with intense ion fluxes with the energy-latitude dispersion typical of the cusp. This is consistent with the magnetic field mapping from the SWFM model run for this event, which indicates that the Polar field line is close to the dayside postnoon magnetopause. The characteristics of this event are distinctly different from other previously reported auroral spots.

[19] *Frey et al.* [2003c] described examples of dayside emissions with similar characteristics, small "spots" observable in the WIC images but not the SI12 (proton aurora) images at latitudes higher than the auroral oval (HiLDA). The events Frey et al. described, which were often long lived, were associated with quiet magnetic conditions and extremely different solar wind conditions from those associated with the 17 August 2001 substorm. The only similarity was the existence of a large positive y component of the interplanetary magnetic field. In addition, *Frey et al.* [2003c] showed that (1) both the simultaneous FAST observations and the examination of model currents and convection from AMIE indicated that the HiLDA electron emissions occurred in a region of upward current that was at higher latitudes than the cusp and that (2) the cusp region was associated with a downward current. On the basis of the conjugate Polar observations in the Southern Hemisphere, we can conclude that this is not the case for the event presented herein, where the upward current was colocated with the cusp-dispersed ion signature.

[20] Although the location of the emission reported herein was similar to that reported for emissions associated with reconnection during large duskward and northward IMF

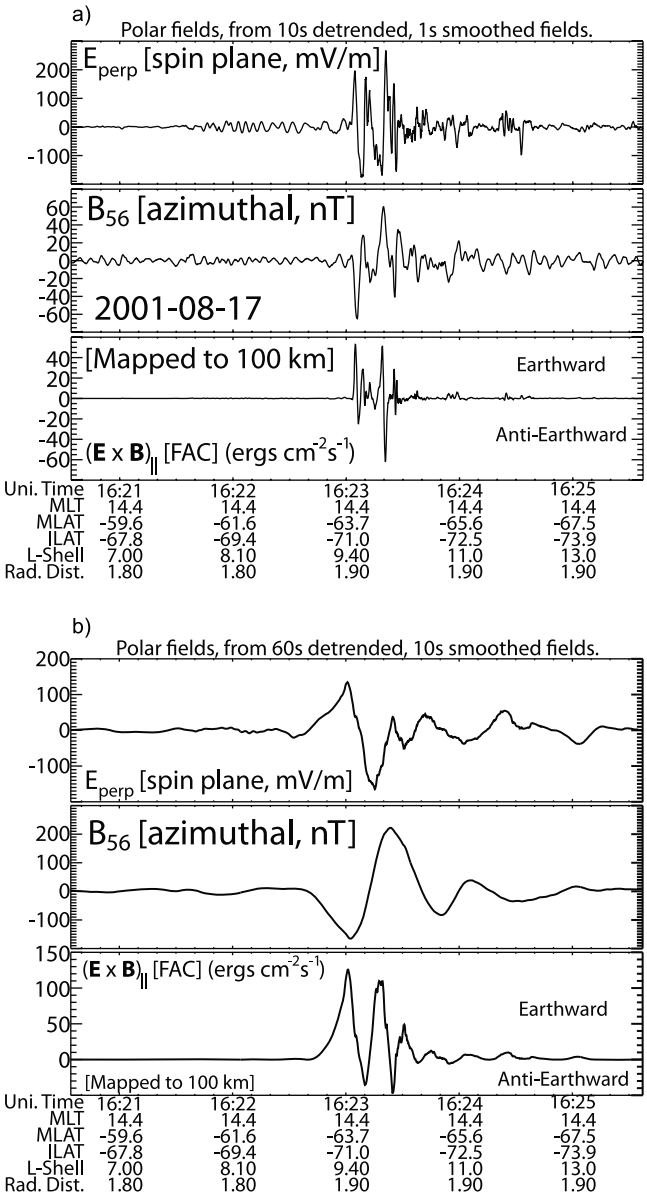

Figure 5. Polar electric and magnetic field data, detrended and filtered to show waves/structures with different time scales. (a) Data detrended at 60 s and smoothed at 10 s: Perpendicular component of the electric field in the spin plane, azimuthal magnetic field, and field-aligned Poynting flux. (b) Data detrended at 10 s and smoothed at 1 s.

[*Frey et al.*, 2002], previously reported emissions at the cusp reconnection foot point contained copious emissions of Lyman alpha, and therefore, they were thought to be primarily due to protons [*Fuselier et al.*, 2002; *Frey et al.*, 2003a]. Typical secondary emission induced auroral emissions were also present, and they were attributed largely to the protons' precipitation, but it is difficult to completely exclude other precipitating particles such as electrons. *Frey et al.* [2003b] extended the study to southward IMF and showed similar dependences of brightness on solar wind pressure and location on B_y and a stronger location dependence on size of IMF B_z. In contrast, the auroral spot described herein was solely electron emissions, and no relationship between solar wind dynamic pressure and brightness was observed. Note that extensive proton emissions were observed at other latitudes and local times during this interval.

[21] A study utilizing a conjunction between Cluster in situ observations of reconnection at the magnetopause and IMAGE observations provided evidence that the protons producing the light seen in the SI12 imager at the foot of the reconnecting field line were accelerated at the reconnection site [*Phan et al.*, 2003]. If the acceleration processes and dynamics occurring between the subsolar magnetopause region and the ionosphere were similar in the Northern and Southern hemispheres in the event described herein, the data from the Polar satellite (at a radial distance of ~1.8 R_E) suggest that the dominant acceleration of the electrons producing the spot occurs well below the magnetopause reconnection region in electric field structures powered by Poynting flux generated in the reconnection process. The assumption that the subsolar reconnection process produces comparable waves and Poynting flux traveling away from the x line toward the Northern and Southern hemispheres seems reasonable.

[22] For the observed solar wind pressure, *Frey et al.* [2003b] would predict the occurrence of a proton emission observable in SI12. Similarly, the observed ion kinetic energy flux at Polar, if mapped to 100 km, is comparable to that shown in Figure 7 of *Frey et al.* [2003b] and would produce an observable emission. There are several possible explanations for this inconsistency. The downward ion kinetic energy flux is in a region of strong upward field-aligned current. If a parallel potential drop is required below the Polar altitude to support this current, the ions would be decelerated, reducing the ion kinetic energy flux and the ion energy below that needed to excite observable emissions. The integrated perpendicular potential drop across the structure is large enough for this to be the case. Because the response of the SI12 camera depends on the proton energy, a decrease in the proton energy could reduce the emission below the observable level [*Frey et al.*, 2003b]. Note that it is also possible that there are significant differences between the auroral emissions in the Northern and Southern hemispheres at the foot of the field line that maps to the magnetopause [*Laundal et al.*, 2010]. The fact that the event occurred near the fall equinox makes this less likely since illumination would be comparable for the two polar caps.

[23] It should also be noted that the spot described herein is poleward of the main oval. It is, therefore, also a very different feature from the "1500 MLT bright spots" described by *Liou et al.* [1999]. Those events were located within the main auroral oval, usually within regions mapping to the plasma sheet. Several bright spots within the main oval and consistent with the event type described by Liou et al. are visible in a number of the images. The bright spots whose occurrence peaked in this local time, described by *Vo and Murphree* [1995], are also different from our event. They usually occurred in a longitudinally spaced series when the solar wind density was low and were interpreted as being due to Kelvin-Helmholtz waves on the magnetopause.

[24] As discussed in section 3, the auroral spot described herein was associated with strong Poynting flux. Comparisons between electron kinetic energy flux, Poynting flux,

and the intensity of auroral emissions have been presented by numerous authors. *Wygant et al.* [2000, 2002] described encounters of Polar with the plasma sheet boundary at ~4 to 6 R_E on the nightside, with in situ measurements of Alfvén waves and Alfvénic Poynting flux and electron kinetic energy flux on field lines mapping to bring aurora. They showed that the observed electron kinetic energy flux was not large enough to produce the aurora observed at the foot of the field line but that the Poynting flux was large enough to provide the energy needed to accelerate the electrons and to account for ion heating and Joule heating in the ionosphere. Simulation studies and comparisons to FAST data for one nightside event [*Chaston et al.*, 2002, Figure 7] indicated that most of the electron acceleration occurred at altitudes near 4000 km. *Chaston et al.* [2003], in a statistical study of FAST observations and comparisons to simulations, provided evidence for acceleration of electrons via Alfvén waves in the cusps at altitudes similar to the event described herein. They also suggested that the waves might be generated in the subsolar reconnection region. *Dombeck et al.* [2005], in a comparison of FAST and Polar data, provided evidence for conversion of Alfvén wave energy to electron kinetic energy between the altitudes of the two satellites. The Polar and IMAGE observations described herein, which suggest that the bulk of the electron acceleration powered by the Poynting flux is occurring at altitudes below 1.8 R_E, are consistent with these studies.

[25] Although it is not possible to determine whether the acceleration of the electrons below the altitude of Polar occurred in a quasi-static parallel potential drop, in a double layer, or in the parallel electric fields associated with kinetic Alfvén waves, the data are most consistent with acceleration due to Alfvén waves. If there was a large parallel potential drop below the satellite, one would expect to see an upflowing ion beam at Polar [see *Paschmann et al.*, 2003; *Ergun et al.*, 2004, and references therein], and this is not observed. As discussed in section 3, the electric and magnetic field data are consistent with kinetic Alfvén waves. The electron distributions are also more consistent with the expectations for Alfvénic acceleration [*Chaston et al.*, 2002, 2003].

[26] *Østgaard et al.* [2009] examined the nightside aurora observed during the event described herein in a study of nightside aurora seen by IMAGE and reconnection events observed by Cluster. They concluded that the electron kinetic energy flux observed at Cluster in association with tail reconnection was not adequate to explain the observed emissions. We note that Alfvénic Poynting flux observed in association with the tail reconnection event on the four Cluster satellites is more than adequate to provide the energy needed for the observed nightside aurora (as shown in Figures 1b and 2). The mapping factor from the Cluster location to 100 km is of the order of 1000, so that the earthward Poynting flux peaks at values of ~500 to 800 mW/m^2. This topic, which is very different from the focus of the work presented herein, will be discussed in more detail in a separate paper.

[27] In summary, the data presented herein are consistent with the hypothesis that the long-lasting electron auroral emission observed by IMAGE maps to the magnetopause region, where reconnection is occurring in association with a large positive IMF B_y and negative IMF B_z and high solar wind density and pressure. This event has many characteristics that are distinctly different from previously reported auroral spots. With the assumption that Polar is on field lines conjugate to the spot, the Polar data suggest that the electrons on these field lines are accelerated by Alfvén waves and/or a quasi-static electric field, primarily at altitudes below the 1.8 R_E altitude of Polar. This can be deduced from the fact that the in situ Poynting flux (mapped to 100 km) is comparable to the energy flux of the emission, while the mapped in situ electron energy flux is much smaller. If the above interpretation is correct, this event provides the first example of auroral electron emission at the foot point of stable dayside reconnection, with electron acceleration occurring at low altitudes due to reconnection-driven Poynting flux.

[28] **Acknowledgments.** This work was supported by NASA grants NNG04GG83G, NNX08AF28G, NNX09AE41G, and NNX08AH84G at University of Minnesota and at University of California, Berkeley, and NASA grants NNX07AL088G and NNX08AQ15G and NSF grant ATM-0802705 at University of Michigan. Work at NCAR was supported in part by NNH09AK621. NCAR is sponsored by the National Science Foundation. Pamela Vo's work on this project was supported by the NSF REU program. We thank J. Scudder for providing the Polar HYDRA data.

[29] Philippa Browning thanks Robert Pfaff and another reviewer for their assistance in evaluating this paper.

References

Akasofu, S.-I. (1964), The development of the auroral substorm, *Planet. Space Sci.*, *12*, 273–282, doi:10.1016/0032-0633(64)90151-5.

Balogh, A., et al. (2001), The Cluster magnetic field investigation: Overview of in-flight performance and initial results, *Ann. Geophys.*, *19*, 1207–1217, doi:10.5194/angeo-19-1207-2001.

Chaston, C. C., J. W. Bonnell, C. W. Carlson, M. Berthomier, L. M. Peticolas, I. Roth, J. P. McFadden, R. E. Ergun, and R. J. Strangeway (2002), Electron acceleration in the ionospheric Alfven resonator, *J. Geophys. Res.*, *107*(A11), 1413, doi:10.1029/2002JA009272.

Chaston, C. C., J. W. Bonnell, C. W. Carlson, J. P. McFadden, R. E. Ergun, and R. J. Strangeway (2003), Properties of small-scale Alfvén waves and accelerated electrons from FAST, *J. Geophys. Res.*, *108*(A4), 8003, doi:10.1029/2002JA009420.

Dombeck, J., C. Cattell, J. R. Wygant, A. Keiling, and J. Scudder (2005), Alfvén waves and Poynting flux observed simultaneously by Polar and FAST in the plasma sheet boundary layer, *J. Geophys. Res.*, *110*, A12S90, doi:10.1029/2005JA011269.

Elphinstone, R. D., J. S. Murphree, and L. L. Cogger (1996), What is a global auroral substorm?, *Rev. Geophys.*, *34*, 169–232, doi:10.1029/96RG00483.

Ergun, R. E., L. Andersson, D. Main, Y.-J. Su, D. L. Newman, M. V. Goldman, C. W. Carlson, A. J. Hull, J. P. McFadden, and F. S. Moser (2004), Auroral particle acceleration by strong double layers: The upward current region, *J. Geophys. Res.*, *109*, A12220, doi:10.1029/2004JA010545.

Frey, H. U. (2007), Localized aurora beyond the auroral oval, *Rev. Geophys.*, *45*, RG1003, doi:10.1029/2005RG000174.

Frey, H. U., S. B. Mende, T. J. Immel, S. A. Fuselier, E. S. Claflin, J.-C. Gérard, and B. Hubert (2002), Proton aurora in the cusp, *J. Geophys. Res.*, *107*(A7), 1091, doi:10.1029/2001JA900161.

Frey, H. U., T. D. Phan, S. A. Fuselier, and S. B. Mende (2003a), Continuous magnetic reconnection at Earth's magnetopause, *Nature*, *426*, 533–537, doi:10.1038/nature02084.

Frey, H. U., S. B. Mende, S. A. Fuselier, T. J. Immel, and N. Østgaard (2003b), Proton aurora in the cusp during southward IMF, *J. Geophys. Res.*, *108*(A7), 1277, doi:10.1029/2003JA009861.

Frey, H. U., T. J. Immel, G. Lu, J. Bonnell, S. A. Fuselier, S. B. Mende, B. Hubert, N. Østgaard, and G. Le (2003c), Properties of localized, high latitude, dayside aurora, *J. Geophys. Res.*, *108*(A4), 8008, doi:10.1029/2002JA009332.

Frey, H. U., N. Østgaard, T. J. Immel, H. Korth, and S. B. Mende (2004), Seasonal dependence of localized, high-latitude dayside aurora (HiLDA), *J. Geophys. Res.*, *109*, A04303, doi:10.1029/2003JA010293.

Fuselier, S. A., H. U. Frey, K. J. Trattner, S. B. Mende, and J. L. Burch (2002), Cusp aurora dependence on interplanetary magnetic field B_z, *J. Geophys. Res.*, *107*(A7), 1111, doi:10.1029/2001JA900165.

Goertz, C. K., and R. W. Boswell (1979), Magnetosphere-ionosphere coupling, *J. Geophys. Res.*, *84*, 7239–7246, doi:10.1029/JA084iA12p07239.

Gombosi, T. I., D. L. De Zeeuw, C. P. Groth, K. G. Powell, C. R. Clauer, and P. Song (2001), From Sun to Earth: Multiscale MHD simulations of space weather, in *Space Weather*, *Geophys. Monogr. Ser.*, vol. 125, edited by P. Song, H. J. Singer, and G. L. Siscoe, pp. 169–176, AGU, Washington, D. C.

Gustafsson, G., et al. (1997), The electric field and wave experiment for the Cluster mission, *Space Sci. Rev.*, *79*, 137–156, doi:10.1023/A:1004975108657.

Harvey, P., et al. (1995), The electric field instrument on the Polar satellite, in *The Global Geospace Mission*, edited by C. T. Russell, pp. 583–596, Kluwer Acad., Dordrecht, Netherlands.

Hones, E. W., Jr. (1976), Observations in the Earth's magnetotail relating to magnetic merging, *Sol. Phys.*, *47*, 101–113, doi:10.1007/BF00152248.

Hull, A. J., J. W. Bonnell, F. S. Mozer, and J. D. Scudder (2003), A statistical study of large-amplitude parallel electric fields in the upward current region of the auroral acceleration region, *J. Geophys. Res.*, *108*(A1), 1007, doi:10.1029/2001JA007540.

Kletzing, C. A. (1994), Electron acceleration by kinetic Alfvén waves, *J. Geophys. Res.*, *99*, 11,095–11,103, doi:10.1029/94JA00345.

Laundal, K. M., N. Østgaard, K. Snekvik, and H. U. Frey (2010), Interhemispheric observations of emerging polar cap asymmetries, *J. Geophys. Res.*, *115*, A07230, doi:10.1029/2009JA015160.

Liou, K., P. T. Newell, C.-I. Meng, T. Sotirelis, M. Brittnacher, and G. Parks (1999), Source region of 1500 MLT auroral bright spots: Simultaneous Polar UV-images and DMSP particle data, *J. Geophys. Res.*, *104*, 24,587–24,602, doi:10.1029/1999JA900290.

Lysak, R. L. (1991), Feedback instability of the ionospheric resonant cavity, *J. Geophys. Res.*, *96*, 1553–1568, doi:10.1029/90JA02154.

Lysak, R. L., and W. Lotko (1996), On the kinetic dispersion relation for shear Alfvén waves, *J. Geophys. Res.*, *101*, 5085–5094, doi:10.1029/95JA03712.

Mende, S. B., et al. (2000), Far ultraviolet imaging from the IMAGE spacecraft, *Space Sci. Rev.*, *91*, 243–270, doi:10.1023/A:1005271728567.

Morooka, M., and T. Mukai (2003), Density as a controlling factor for seasonal and altitudinal variations of the auroral particle acceleration region, *J. Geophys. Res.*, *108*(A7), 1306, doi:10.1029/2002JA009786.

Østgaard, N., K. Snekvik, A. L. Borg, A. Asnes, A. Pedersen, M. Øieroset, T. Phan, and S. E. Haaland (2009), Can magnetotail reconnection produce the auroral intensities observed in the conjugate ionosphere?, *J. Geophys. Res.*, *114*, A06204, doi:10.1029/2009JA014185.

Paschmann, G., S. Haaland, and R. A. Treumann (Eds.) (2003), *Auroral Plasma Physics*, Kluwer Acad., Dordrecht, Netherlands.

Phan, T., et al. (2003), Simultaneous Cluster and IMAGE observations of cusp reconnection and auroral proton spot for northward IMF, *Geophys. Res. Lett.*, *30*(10), 1509, doi:10.1029/2003GL016885.

Reiff, P., T. W. Hill, and J. L. Burch (1977), Solar wind plasma injection at the dayside magnetospheric cusp, *J. Geophys. Res.*, *82*, 479–491, doi:10.1029/JA082i004p00479.

Réme, H., et al. (1997), The Cluster Ion Spectrometry (CIS) experiment, *Space Sci. Rev.*, *79*, 303–350, doi:10.1023/A:1004929816409.

Richmond, A. D. (1992), Assimilative mapping of ionospheric electrodynamics, *Adv. Space Res.*, *12*, 59–68.

Richmond, A. D., G. Lu, B. A. Emery, and D. J. Knipp (1998), The AMIE procedure: Prospects for space weather specification and prediction, *Adv. Space Res.*, *22*, 103–112, doi:10.1016/S0273-1177(97)01108-3.

Russell, C. T., et al. (1995), The GGS/Polar magnetic fields investigation, in *The Global Geospace Mission*, edited by C. T. Russell, pp. 563–582, Kluwer Acad., Dordrecht, Netherlands.

Scudder, J., et al. (1995), HYDRA—A 3-dimensional electron and ion hot plasma instrument for the Polar spacecraft of the GGS mission, in *The Global Geospace Mission*, edited by C. T. Russell, pp. 459–495, Kluwer Acad., Dordrecht, Netherlands.

Smith, M. F., and M. Lockwood (1996), Earth's magnetospheric cusps, *Rev. Geophys.*, *34*, 233–260, doi:10.1029/96RG00893.

Tóth, G., et al. (2005), Space Weather Modeling Framework: A new tool for the space science community, *J. Geophys. Res.*, *110*, A12226, doi:10.1029/2005JA011126.

Vo, H. B., and J. S. Murphree (1995), A study of dayside auroral bright spots seen by the Viking auroral imager, *J. Geophys. Res.*, *100*, 3649–3655, doi:10.1029/94JA03138.

Wygant, J. R., et al. (2000), Polar spacecraft based comparisons of intense electric fields and Poynting flux near and within the plasma sheet-tail lobe boundary to UVI images: An energy source for the aurora, *J. Geophys. Res.*, *105*, 18,675–18,692, doi:10.1029/1999JA900500.

Wygant, J. R., et al. (2002), Evidence for kinetic Alfvén waves and parallel electron energization at 4–6 R_E altitudes in the plasma sheet boundary layer, *J. Geophys. Res.*, *107*(A8), 1201, doi:10.1029/2001JA900113.

C. Cattell, J. Dombeck, A. Preiwisch, S. Thaller, P. Vo, L. B. Wilson III, and J. Wygant, School of Physics and Astronomy, University of Minnesota, Twin Cities, Minneapolis, MN 55455, USA. (cattell@fields.space.umn.edu)

H. U. Frey and S. B. Mende, Space Sciences Laboratory, University of California, Berkeley, CA 94720, USA.

R. Ilie, Department of Atmospheric, Oceanic and Space Sciences, University of Michigan, Ann Arbor, MI 48109, USA.

G. Lu, High Altitude Observatory, National Center for Atmospheric Research, Boulder, CO 80307, USA.